Journal of Physics: Conference Series **551** (2014) 012032 doi:10.1088/1742-6596/551/1/012032

β-NMR of $^8Li^+$ in rutile TiO_2

R M L McFadden[1], D L Cortie[1,2,3], D J Arseneau[4], T J Buck[2], C-C Chen[5], M H Dehn[6], S R Dunsiger[6], R F Kiefl[2], C D P Levy[4], C Li[7], G D Morris[4], M R Pearson[4], D Samuelis[5], J Xiao[1], J Maier[5] and W A MacFarlane[1]

[1] Department of Chemistry, University of British Columbia, 2036 Main Mall, Vancouver, BC V6T 1Z1, Canada
[2] Department of Physics and Astronomy, University of British Columbia, 6224 Agricultural Road, Vancouver, BC V6T 1Z1, Canada
[3] Quantum Matter Institute, University of British Columbia, Vancouver, BC V6T 1Z4
[4] TRIUMF, 4004 Wesbrook Mall, Vancouver, BC V6T 2A3, Canada
[5] Max-Planck-Institut für Festkörperforschung, D-70569 Stuttgart, Germany
[6] Physik-Department, Technische Universität München, James-Franck-Straße 1, 85748 Garching bei München, Germany
[7] Shanghai Institute of Ceramics, Chinese Academy of Sciences, 1295 Dingxi Road, Shanghai, P.R. China 200050

E-mail: wam@chem.ubc.ca

Abstract. We report preliminary low-energy β-NMR measurements of $^8Li^+$ implanted in single crystal rutile TiO_2 at an applied field of 6.55 T and 300 K. We observe a broad 12 kHz wide quadrupole split resonance with unresolved features and a sharp component at the Larmor frequency. The line broadening may be caused by overlapping multi-quantum transitions or motion of $^8Li^+$ on the scale of its lifetime (1.21 s). We also find spin-lattice relaxation that is relatively fast compared to other wide band gap insulators. The origin of this fast relaxation is also likely quadrupolar and may be due to anisotropic $^8Li^+$ diffusion.

1. Introduction

Like the many TiO_2 polymorphs, rutile has applications as an anode material in lithium-ion batteries [1, 2]. Its tetragonal structure is comprised of edge-sharing TiO_6 octahedra that extend along the c-axis, forming natural channels which Li can occupy during electrochemical intercalation. For incorporation into functional devices, a detailed understanding of the diffusivity of Li^+ is necessary. Macroscopic methods (e.g., impedance spectroscopy) are often used to probe ionic diffusion, but are unable to distinguish between different conductive pathways. The applicability of NMR to probe dynamics in solids is well known [3], and can be especially useful in resolving multiple diffusive pathways activated in different thermal regions [4]. Li dynamics in TiO_2 polymorphs (and related compounds) have been studied by conventional NMR [5, 6, 7, 8, 9, 10], but no such investigation has been undertaken for rutile. We report here a preliminary look at Li^+ implanted (i.e., not doped) in rutile titania using beta-detected NMR (β-NMR) at room temperature and high magnetic field.

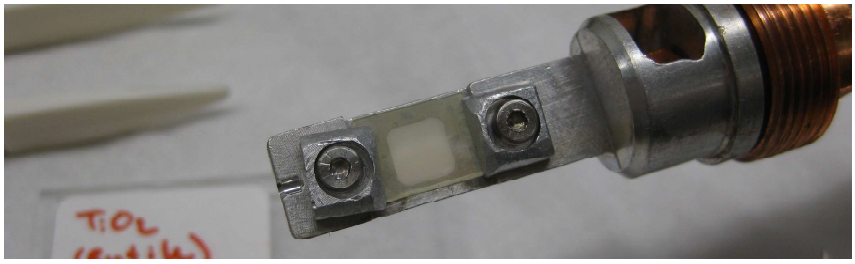

Figure 1. Cleaved rutile TiO_2 (100) substrate from Crystal GmbH mounted in the β-NMR sample holder. The pale yellow colour is indicative of a minor presence of defects.

2. Experimental

A 10 mm × 10 mm single crystal rutile TiO_2 (100) substrate was purchased from Crystal GmbH. The rutile polymorph is tetragonal ($a = b = 0.4584$ nm, $c = 0.2953$ nm) with space group $P4_2/mnm$. The substrate appears transparent pale yellow in colour, qualitatively indicating a minor presence of defects [11]. The sample was cleaved for mounting on a cold finger cryostat (see Figure 1).

β-NMR experiments were performed at TRIUMF's Isotope Separator and Accelerator (ISAC) facility using a low-energy ($\sim$ 20 keV) radioactive beam of spin-polarized $^8Li^+$ with a typical flux of $\sim 10^6$ ions s^{-1} and spot size of $\sim$ 2 mm in diameter. The probe nucleus, ^{8}Li, has spin $I = 2$, a quadrupole moment $Q = +31.4$ mb, a gyromagnetic ratio $\gamma = 6.3015$ MHz T^{-1}, and a mean lifetime $\tau = 1.21$ s. A large nuclear spin-polarization ($\sim$ 70%) is achieved by collinear optical pumping with resonant circularly polarized laser light [12] such that the direction of spin-polarization is aligned parallel or antiparallel to the static applied magnetic field, B_0. A high-voltage bias is used to decelerate the beam prior to implantation. Depth-profiles were estimated from Monte Carlo simulations of 10^6 ions using SRIM [13] (see Figure 2). Details of the spectrometer can be found elsewhere [14, 15].

Resonance measurements were performed using a continuous $^8Li^+$ beam with a transverse RF-field H_1 operated in continuous wave (CW) mode. Application of an RF-field at the appropriate

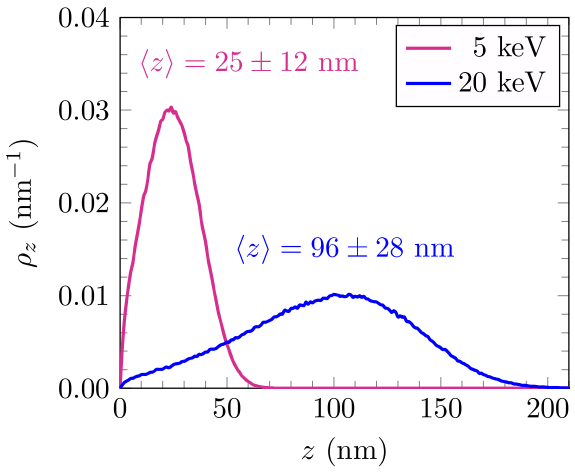

Figure 2. SRIM stopping profiles for 10^6 $^8Li^+$ ions implanted in TiO_2, histogrammed into 1 nm wide bins. Here, z is the distance from the substrate surface and ρ_z is the stopping probability density. Mean and root mean square implantation depths are inset over the profiles.

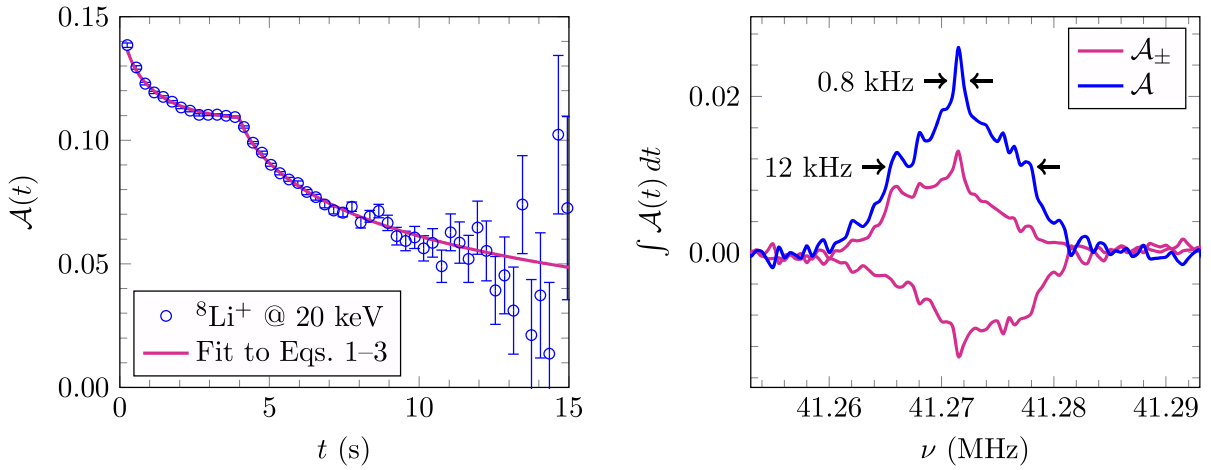

Figure 3. β-NMR spectra of ^{8}Li$^+$ implanted in rutile TiO_2 (100) at 20 keV and 300 K. *Left*: Spin-lattice relaxation — time-differential asymmetry showing the temporal evolution of ^{8}Li$^+$ spin-polarization. *Right*: CW resonance spectra — time-integrated asymmetry of the positive and negative helicities, $\mathcal{A}_\pm$, and the combined asymmetry, $\mathcal{A}$, from both helicities.

resonant frequency causes rapid ^{8}Li spin-precession perpendicular to the H_1 field-axis, destroying ^{8}Li polarization, observed as a change in time-integrated asymmetry. Spin-lattice relaxation (SLR) measurements were performed using a pulsed beam and no RF-field. The time-differential asymmetry, which is proportional to ^{8}Li spin-polarization, is monitored both during and following a 4 second ^{8}Li$^+$ beam pulse. All measurements were performed in a static magnetic field $B_0 = 6.55$ T $\parallel$ the rutile TiO_2 (100) (i.e., the a-axis).

3. Results & Discussion

Figure 3 (*left*) shows the spin-lattice relaxation (SLR) spectrum at 300 K of ^{8}Li$^+$ implanted in rutile TiO_2 at 20 keV. The time-evolution of ^{8}Li$^+$ asymmetry follows [16]:

$$\mathcal{A}(t) = \frac{\int_0^t \exp\left[-\left(t-t'\right)/\tau\right] f\left(t,t';T_1\right)\,dt'}{\int_0^t \exp\left[-t'/\tau\right]\,dt'} \qquad t \le \Delta \tag{1}$$

$$= \frac{\int_0^\Delta \exp\left[-\left(\Delta-t'\right)/\tau\right] f\left(t,t';T_1\right)\,dt'}{\int_0^\Delta \exp\left[-t'/\tau\right]\,dt'} \qquad t > \Delta \tag{2}$$

where τ is the mean lifetime of ^{8}Li, and Δ is the duration of the beam pulse, corresponding to the pronounced kink at $t = 4$ s. $f\left(t,t';T_1\right)$ is the longitudinal relaxation function phenomenologically defined as a stretched exponential:

$$f\left(t,t';T_1\right) = \mathcal{A}_0 \exp\left[-\left\{\left(t-t'\right)/T_1\right\}^\beta\right], \tag{3}$$

where $\mathcal{A}_0$, T_1, and β are the initial asymmetry, SLR relaxation time, and stretching exponent ($0 \le \beta \le 1$). A best fit of Eqs. 1–3 to the SLR spectra in Figure 3 (*left*) yields: $\mathcal{A}_0 = 0.166 \pm 0.004$, $\beta = 0.386 \pm 0.020$, and $T_1^{-1} = 0.141 \pm 0.005$ s^{-1}. Such a relaxation rate is relatively high compared to other insulating metal oxides [17], where ^{8}Li$^+$ can be nearly non-relaxing.[1] As rutile is non-cubic and virtually without nuclear moments (^{47}Ti: $I = 3/2$, 7.28%; ^{49}Ti: $I = 5/2$,

[1] See e.g., W A MacFarlane et al. and Z Salman et al. in these proceedings.

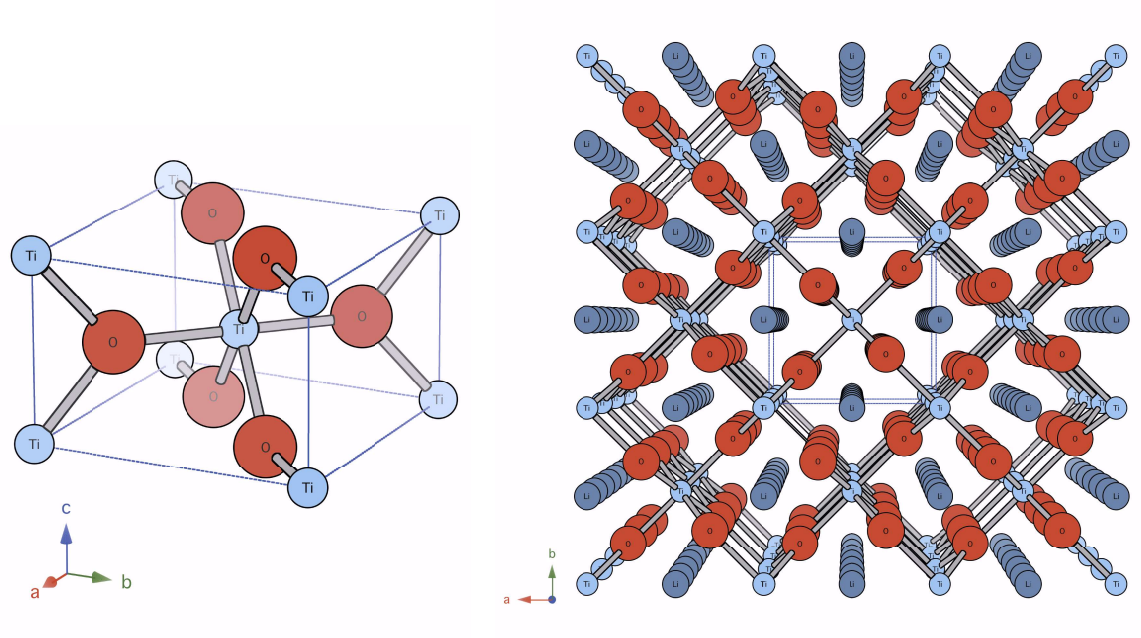

Figure 4. Crystal structure of rutile TiO_2 — oxygen and titanium atoms appear as red and light blue spheres, with bonded atoms connected by grey cylinders. *Left*: Unit cell. *Right*: View along the c-axis of a 3×3 rutile supercell. Octahedral Li sites are shown as dark blue spheres and the dashed blue line encloses the unit cell.

5.51%, ^{17}O: $I = 5/2$, 0.038%), it is likely that the relaxation is predominantly quadrupolar in nature. It is worth noting that a previous β-NMR investigation of $^{8}Li^{+}$ in rutile TiO_2 reported a 30% preservation of nuclear spin-polarization at low magnetic fields in stark contrast to 100% retention for other implanted nuclear probes (e.g., ^{12}B) [18]. This is consistent with our observation of appreciable $^{8}Li^{+}$ relaxation. Additionally, we find a depth dependence to the spin-lattice relaxation rate at 300 K, with T_1^{-1} decreasing by a factor of ~ 5 when the implantation energy is decreased from 20 keV to 5 keV. The origin of this depth-dependence is not well-understood at this time.

A CW resonance spectrum of 20 keV $^{8}Li^{+}$ implanted in rutile TiO_2 at 300 K is shown in Figure 3 (*right*). The asymmetric time-integrated asymmetries from spin-polarization with different helicities ($\mathcal{A}_{\pm}$) are characteristic of a quadrupole split resonance [17, 19]. From the combined asymmetry ($\mathcal{A}$), we find a broad, 12.48 ± 0.12 kHz wide quadrupole split resonance with unresolved features. This is in stark contrast to the $^{8}Li^{+}$ resonance in Bi, where the four quadrupole satellite and three double-quantum transitions are well-resolved,[2] or in the perovskite $SrTiO_3$, where the satellite splitting is greater by about an order of magnitude [17]. X-ray diffraction and reflectometry measurements do not reveal the presence of impurity phases, though static disorder (e.g., from oxygen vacancies, as indicated by the discolouration of the crystal, or transition metal impurities) is a possible cause for the broadening. A sharp, large amplitude, 0.76 ± 0.05 kHz wide resonance is also observed at the Larmor frequency, $\nu_0 = 41.2715$ MHz. This may be a multi-quantum transition (e.g., the double-quantum $|\Delta m| = 2$ transition between $m = \pm 1$ states). Such transitions appear as large sharp (narrow) enhancements in the resonance spectrum and can be especially prevalent in CW β-NMR, where strong RF fields are often used [20], as is the case here. This can easily be tested by comparing spectra at different

[2] See W A MacFarlane et al. in these proceedings.

values of the RF magnetic field amplitude H_1. A multiquantum resonance will be attenuated very strongly by a reduced H_1.

Another possibility is that the observed pattern is due to Li residing in multiple sites with overlapping resonances. Molecular dynamics (MD) and density functional theory (DFT) calculations of lithiated rutile (Li_xTiO_2: $0 < x \leq 1$) [21, 22, 23, 24, 25] predict preferential sites for lithium at octahedral and tetrahedral oxygen-coordinated interstitial sites. Figure 4 shows the octahedral site for Li along the rutile c-axis, which is predicted to be energetically favourable over the tetrahedral site by ~ 0.8 eV [21, 22].

It is also possible that the sharp component of the resonance in Figure 3 (*right*) is from a motionally narrowed fraction of $^8Li^+$, as it experiences an average electric field gradient (EFG) from site hopping during its lifetime. MD and DFT calculations also predict fast, anisotropic 1D diffusion of Li^+ along the rutile c-axis with a low hopping-barrier of ~ 0.05 eV [21, 22, 24, 25].[3] These barriers are significantly lower than what is observed experimentally from macroscopic methods [26, 27], though such measurements are done far from the limit of infinitely dilute lithium, where the potential energy landscape is likely altered by lattice distortions and Li^+–Li^+ interactions [22, 28]. The broad component of the resonance may be due to fast-diffusion of $^8Li^+$ to Frenkel pairs, formed from irradiation, before they heal. Motion of $^8Li^+$ during its lifetime may also explain the relatively large SLR rate observed and measuring its temperature dependence would be a way of testing this. It will be interesting to see if the predicted low-barrier hopping can be probed with β-NMR, which is uniquely suited for diffusion measurements at such dilute lithium concentrations.

4. Summary

In a preliminary study of $^8Li^+$ in rutile TiO_2 at 300 K and $B_0 = 6.55$ T $\parallel$ the rutile (100) using β-NMR, we find a relatively fast relaxation compared to other wide band gap insulators and an unresolved quadrupole split resonance in contrast to well-resolved quadrupolar patterns in other materials. We propose that these may be due to motion of $^8Li^+$ during its lifetime. A full temperature scan of SLR rates and resonance lineshapes (at different RF powers) in future experiments will help determine the relaxation mechanism and elucidate the behaviour of Li^+ in rutile titania.

References

[1] Hu Y S, Kienle L, Guo Y G and Maier J 2006 *Adv. Mater.* **18** 1421–1426
[2] Reddy M V, Subba Rao G V and Chowdari B V R 2013 *Chem. Rev.* **113** 5364–5457
[3] Kuhn A, Kunze M, Sreeraj P, Wiemhöfer H D, Thangadurai V, Wilkening M and Heitjans P 2012 *Solid State Nucl. Magn. Reson.* **42** 2–8
[4] Kuhn A, Sreeraj P, Pöttgen R, Wiemhöfer H D, Wilkening M and Heitjans P 2011 *J. Am. Chem. Soc.* **133** 11018–11021
[5] Wagemaker M, van de Krol R, Kentgens A P M, van Well A A and Mulder F M 2001 *J. Am. Chem. Soc.* **123** 11454–11461
[6] Wagemaker M, Kentgens A P M and Mulder F M 2002 *Nature* **418** 397–399
[7] Wilkening M, Amade R, Iwaniak W and Heitjans P 2007 *Phys. Chem. Chem. Phys.* **9** 1239–1246
[8] Wilkening M, Iwaniak W, Heine J, Epp V, Kleinert A, Behrens M, Nuspl G, Bensch W and Heitjans P 2007 *Phys. Chem. Chem. Phys.* **9** 6199–6202
[9] Wilkening M, Lyness C, Armstrong A R and Bruce P G 2009 *J. Phys. Chem.* C **113** 4741–4744
[10] Bottke P, Ren Y, Hanzu I, Bruce P G and Wilkening M 2014 *Phys. Chem. Chem. Phys.* **16** 1894–1901
[11] Diebold U 2003 *Surf. Sci. Rep.* **48** 53–229
[12] Levy C D P, Pearson M R, Kiefl R F, Mané E, Morris G D and Voss A 2014 *Hyperfine Interact.* **225** 165–172
[13] Ziegler J F, Ziegler M and Biersack J 2010 *Nucl. Instrum. Methods Phys. Res.* B **268** 1818–1823
[14] Morris G D, MacFarlane W A, Chow K H, Salman Z, Arseneau D J, Daviel S, Hatakeyama A, Kreitzman

[3] Barriers for diffusion in the *ab*-plane are predicted to be larger by an order of magnitude.

S R, Levy C D P, Poutissou R, Heffner R H, Elenewski J E, Greene L H and Kiefl R F 2004 *Phys. Rev. Lett.* **93** 157601
[15] Morris G D 2014 *Hyperfine Interact.* **225** 173–182
[16] Salman Z, Kiefl R F, Chow K H, Hossain M D, Keeler T A, Kreitzman S R, Levy C D P, Miller R I, Parolin T J, Pearson M R, Saadaoui H, Schultz J D, Smadella M, Wang D and MacFarlane W A 2006 *Phys. Rev. Lett.* **96** 147601
[17] MacFarlane W A, Morris G D, Chow K H, Baartman R A, Daviel S, Dunsiger S, Hatakeyama A, Kreitzman S, Levy C, Miller R, Nichol K, Poutissou R, Dumont E, Greene L H and Kiefl R F 2003 *Physica* B **326** 209–212
[18] Ogura M, Minamisono K, Sumikama T, Nagatomo T, Iwakoshi T, Miyake T, Hashimoto K, Kudo S, Arimura K, Ota M, Akutsu K, Sato K, Mihara M, Fukuda M, Matsuta K, Akai H and Minamisono T 2001 *Hyperfine Interact.* **136–137** 195–199
[19] Parolin T J, Shi J, Salman Z, Chow K H, Dosanjh P, Saadaoui H, Song Q, Hossain M D, Kiefl R F, Levy C D P, Pearson M R and MacFarlane W A 2009 *Phys. Rev.* B **80** 174109
[20] Dubbers D, Dörr K, Ackermann H, Fujara F, Grupp H, Grupp M, Heitjans P, Körblein A and Stöckmann H J 1977 *Z. Phys.* A **282** 243–248
[21] Koudriachova M V, Harrison N M and de Leeuw S W 2001 *Phys. Rev. Lett.* **86** 1275–1278
[22] Koudriachova M V, Harrison N M and de Leeuw S W 2002 *Phys. Rev.* B **65** 235423
[23] Koudriachova M V, Harrison N M and de Leeuw S W 2003 *Solid State Ionics* **157** 35–38
[24] Kerisit S, Rosso K M, Yang Z and Liu J 2009 *J. Phys. Chem.* C **113** 20998–21007
[25] Yildirim H, Greeley J P and Sankaranarayanan S K R S 2012 *Phys. Chem. Chem. Phys.* **14** 4565–4576
[26] Johnson O W 1964 *Phys. Rev.* **136** A284–A290
[27] Bach S, Pereira-Ramos J and Willman P 2010 *Electrochim. Acta* **55** 4952–4959
[28] Koudriachova M V, Harrison N M and de Leeuw S W 2002 *Comput. Mater. Sci.* **24** 235–240